SINTEZA ȘI EVALUAREA SCAFFOLDURILOR COMPOZITE PE BAZĂ DE FIBRE DE PVDF ȘI PULBERI MINERALE PENTRU APLICAȚII MEDICALE

SYNTHESIS AND EVALUATION OF COMPOSITE SCAFFOLDS BASED ON PVDF FIBRES AND MINERAL POWDERS FOR MEDICAL APPLICATIONS

ANDRADA-ELENA ALECU [1], STEFANIA-ANDREEA GÎRJOABĂ [1], MIHAELA BEREGOI [2*], MIHAELA BACALUM [3], MINA RAILEANU [3], SORIN-ION JINGA [1], CRISTINA BUSUIOC[1]

[1] *University POLITEHNICA of Bucharest, RO-060042, Bucharest, ROMANIA*
[2] *National Institute of Materials Physics, RO-077125, Măgurele, ROMANIA*
[3] *Horia Hulubei National Institute for Physics and Nuclear Engineering, RO-077125, Măgurele, ROMANIA*

In this work, polyvinylidene fluoride (PVDF) fibres loaded with mineral powders, such as titanium dioxide (TiO_2), barium titanate ($BaTiO_3$), and calcium magnesium silicate ($Ca_xMgSi_2O_y$), were prepared by electrospinning polymeric suspensions containing 20 wt.% PVDF and 3 wt.% powder. The piezoelectric polymer was combined with powders having antibacterial, piezoelectric, or bioactive properties, respectively, in the desire to obtain multifunctional materials compatible with the requirements of the medical field. All powders were characterized in terms of morphology and crystalline structure, which confirmed the nanometric character of TiO_2 samples and micrometric one for the other two, as well as the lower crystallite size for TiO_2 specimens as against $BaTiO_3$ and $Ca_xMgSi_2O_y$. The final fibrous scaffolds were homogeneous, composed of individual fibres with a diameter below 1 μm and decorated with aggregates of inorganic particles, placed either inside the fibres or attached to their surface. The biological evaluation demonstrated the superiority of the composites towards the plain polymer in terms of cell viability.

În această lucrare, fibrele de fluorură de poliviniliden (PVDF) încărcate cu pulberi minerale, cum ar fi dioxid de titan (TiO_2), titanat de bariu ($BaTiO_3$) și silicat de calciu și magneziu ($Ca_xMgSi_2O_y$), au fost preparate prin electrofilarea de suspensii polimerice conținând 20 %grav PVDF și 3 %grav pulbere. Polimerul piezoelectric a fost combinat cu pulberi având proprietăți antibacteriene, piezoelectrice, respectiv bioactive, din dorința de a obține materiale multifuncționale compatibile cu cerințele domeniului medical. Toate pulberile au fost caracterizate din punctul de vedere al morfologiei și structurii cristaline, ceea ce a confirmat caracterul nanometric al probelor de TiO_2 și cel micrometric pentru celelalte două, precum și dimensiunea de cristalit mai mică pentru specimenele de TiO_2 față de $BaTiO_3$ și $Ca_xMgSi_2O_y$. Scaffoldurile fibroase finale au fost omogene, compuse din fibre individuale cu diametru sub 1 μm și decorate cu agregate de particule anorganice, plasate fie în interiorul fibrelor, fie atașate la suprafața acestora. Evaluarea biologică a demonstrat superioritatea compozitelor față de polimerul simplu în ceea ce privește viabilitatea celulară.

Keywords: *Polyvinylidene fluoride; Titanium dioxide; Barium titanate; Akermanite; Electrospinning; Tissue Engineering.*

1.Introduction

Tissue engineering represents the combination of two increasingly studied fields of research, materials engineering, and medical engineering, which lead to the development of materials that can be used to obtain potential substitutes for biological tissue [1, 2, 3]. Thus, the corresponding researchers have studied materials belonging to different classes in their attempt to find the best combinations that lead to optimized properties. Considering the category of inorganic materials, these were mostly approached for solving hard tissue-related problems, such as small, localized defects or extended defects generated by trauma or resections. Therefore, systems like calcium phosphates [4], simple or mixed oxides [5, 6], and even complex compounds from the class of silicates [7] were extensively integrated into applications for which biocompatibility is a key feature. For example, the *in vivo* tests performed on calcium pyrophosphate ($Ca_2P_2O_7$) demonstrated that it can be recommended for the regenerative treatment of bone defects [8]. It was also reported that the scaffolds made of calcium orthophosphate ($CaPO_4$) induce bone formation and vascularization [9]. Switching to oxides, these were mostly approached as active phases, which could either confer antibacterial properties to the bone substitute matrix or open the possibility of external control through controllable stimuli. Titanium dioxide (TiO_2) can be included in the first situation, since it showed strong antibacterial potential against both Gram-negative and positive bacteria and antioxidant activity [10], while barium titanate ($BaTiO_3$) was proven to possess piezoelectric properties comparable to dry bone [11] or ferromagnetic features which allows the development of personalized implants by controlling the local magnetic response through the applied field and spatial arrangement [12]. The third important family of compounds is that of calcium magnesium silicates

* Autor corespondent/*Corresponding author*,
E-mail: mihaela.oancea@infim.ro

(CMS), which were recently loaded on polycaprolactone fibres, resulting in cell-friendly supports with a better cellular proliferation as the powder concentration increases and enhanced bioactivity with calcium content growth [13].

In the field of tissue engineering and regenerative engineering, polymers are also of real interest. Due to its unique mechanical properties, polyvinylidene fluoride (PVDF, $(C_2H_2F_2)_n$) is considered among the most important synthetic polymers [14]. PVDF is a semi-crystalline, flexible polymer [15], with thermal and chemical stability [16], biocompatibility, and resistance to aging over time [17]. It has five polar and non-polar phases: *α*, *β*, *γ*, *ε,* and *δ* [18]; from them all, the *β* phase is the best for demonstrating its excellent piezoelectric and pyroelectric properties [19, 20], therefore it can be integrated into various applications, such as electronics [21], energy storage [17], sensors [22] and medical devices [23]. Several researchers have already demonstrated the potential of PVDF-based materials for the design of wearable sensors and human energy harvesters [24]. In terms of tissue engineering purposes, it has been shown that electrosprayed PVDF substrates naturally induce human mesenchymal stem cell differentiation into other lineages when chemically stimulated [25]. PVDF was also employed for the fabrication of an intestinal sleeve implant, being concluded that the films inserted in the digestive tract of rats for the treatment of type 2 diabetes show potential for the control of these diseases [26].

The electrospinning method is the best one for obtaining fibres due to the adjustable parameters [27] and the results obtained [28], namely long and continuous fibres [29], with different diameters [30]. After analysing the influence of the processing parameters on the morpho-structural and electrical properties of PVDF fibrous layers, Castkova *et al.* [31] revealed that the mean fibre diameter decreases and β phase content increases as the applied voltage rises; moreover, the piezoelectric activity was higher in the transversal direction than in the longitudinal one. When combined with silver nanoparticles, PVDF electrospun mats exhibited higher permittivity due to the conductive nature of the metal and improved interfacial polarization; such behaviour recommends these composites for applications such as supercapacitors, nanogenerators and self-powering devices [32]. Sta. Agueda *et al.* [33] also studied PVDF fibres synthesized by electrospinning, the promising mechanical integrity of the corresponding scaffolds offering the opportunity to develop an alternative treatment for End Stage Renal Disease.

PVDF fibres are used in the medical field either as unitary systems or for obtaining composite materials. Some researchers reported the obtaining of bifunctional PVDF/TiO_2 fibrous scaffolds by electrostatic spinning technology and hydrothermal reaction method; these presented high efficiency in oil/water emulsion separation and excellent photocatalytic degradation performance of organic dyes [34]. Arif *et al.* [1] also prepared PVDF/TiO_2 composite membranes by a phase-inversion technique and demonstrated their antibacterial activity generated by TiO_2 nanoparticles; briefly, the growth rate of *E. coli* decreased dramatically with the increase of TiO_2 loading, but a too high concentration of oxide could lead to particle agglomeration and subsequently to fewer active sites for bacteria killing. On another hand, Su *et al.* [35] showed that the dielectric properties of PDVF/$BaTiO_3$ composite membranes with finger-like pore structure are increased thanks to $BaTiO_3$ nanoparticles incorporation in PVDF membranes processed by a non-solvent induced phase separation, even though the particles were not dispersed uniformly; the compatibility and dispersion were enhanced by using a silane coupling agent. Another group tried to mimic the extracellular matrix and enhance the piezoelectric response, so he proposed PVDF/$BaTiO_3$ fibrous scaffolds fabricated by electrospinning onto a rotating drum to promote the fibre alignment and embedding micro- and nanosized tetragonal $BaTiO_3$ particles; the presence of $BaTiO_3$ powder led to a decrease in fibre diameter and superficial charge density but also hindered the bioactivity of PVDF fibres [36]. Moreover, Rodrigues *et al.* [37] developed PVDF/nano-hydroxyapatite (nHAp) fibrous scaffolds by electrospinning the polymer, modifying the surface by oxygen plasma treatment and electrodepositing nHAp; the slight reduction in thermal stability was counterbalanced by the important bactericidal and bioactive properties, as well as the high osteoblasts viability, making them a feasible alternative for bone grafts. When it comes to the combination of PVDF with silicates, no paper was found in the scientific literature. There are only some studies regarding the development of PVDF/SiO_2 composite membranes. One of them describes the production of such materials by a non-solvent thermally induced phase separation method, which allows the tunning of membrane morphology and pore structure, resulting in high-performance systems suitable for oil/water emulsion separation [38].

The present work reports on the integration of titanium dioxide (TiO_2), barium titanate ($BaTiO_3$), and calcium magnesium silicate ($Ca_xMgSi_2O_y$) powders into polyvinylidene fluoride (PVDF) fibres through the electrospinning technique. Afterward, the samples were analysed from physicochemical and biological point of view to determine their potential for the development of specific medical applications. Such combinations between polymeric and mineral phases, processed in the form of one-dimensional structures, have been addressed to a small extent by now, which gives us the opportunity to propose new and improved biomaterials with multifunctional properties.

2. Materials and methods

2.1.Materials

The mineral powders were synthesized by wet-chemistry methods, as follows: titanium dioxide (TiO_2) by sol-gel (T-sg) and precipitation (T-pp), calcium magnesium silicate (A, starting from akermanite oxide composition) by sol-gel, while barium titanate ($BaTiO_3$, BT, 99 %, particles < 3 μm, Sigma-Aldrich) was commercially available. The details of all routes are given in [39] for TiO_2 and [40] for A. Briefly, titanium(IV) isopropoxide (Ti(O-i-Pr)4, 97 %, ρ = 0.96 g/mL, Sigma-Aldrich, Burlington, MA, USA) and isopropyl alcohol (i-PrOH, ≥ 98 %) were used as Ti precursor and solvent, with nitric acid (HNO_3) for pH adjustment in the case of sol-gel method and calcination at 500 °C for both situations. On the other hand, calcium nitrate tetrahydrate ($Ca(NO_3)_2{\cdot}4H_2O$, 99 %, Sigma-Aldrich, Burlington, MA, USA), magnesium nitrate hexahydrate ($Mg(NO_3)_2{\cdot}6H_2O$, 99 %, Sigma-Aldrich, Burlington, MA, USA) and tetraethyl orthosilicate ($Si(OEt)_4$, TEOS, 98 %, Sigma-Aldrich, Burlington, MA, USA) were used as cationic precursors, with nitric acid (HNO_3) as pH regulator and thermal treatment at 1300 °C.

Polyvinylidene fluoride (PVDF, $(CH_2CF_2)_n$, 275.000 g/mol, Sigma-Aldrich, Burlington, MA, USA), dimethylformamide (DMF, $HCON(CH_3)_2$, ≥ 99.9 %, Sigma-Aldrich, Burlington, MA, USA) and acetone (Ac, CH_3COCH_3, ≥ 99.9 %, Sigma-Aldrich, Burlington, MA, USA) were employed as polymer and solvents for the fibres fabrication.

2.2.Methods

The electrospinning approach was selected for the obtaining of fibres based on PVDF and inorganic powders (T-sg, T-pp, BT, A). First, 3 wt% powder was dispersed in the solvent mixture (DMF:Ac = 2:3) by ultrasonication for 10 min; then, 20 wt% PVDF was added and solubilised by magnetic stirring for 3 h, at 80 °C. The solvent ratio and polymer concentration were chosen after an extended study previously performed by our research group [6]. Thus, DMF as a single solvent or the combination of DMF with dimethyl sulfoxide did not allow the formation of one-dimensional structures, while a ratio of 1:1 or 4:1 between DMF and Ac led to beaded fibres or favoured the electrospraying process instead of electrospinning. However, the increase of PVDF concentration up to 20 % always had a beneficial impact on diameter constancy over long distance. The homogenised solutions were electrospun using as spinneret a blunt tip stainless steel needle with an inner diameter of 0.8 mm and applying the following conditions: 1 mL/h feeding rate, 18 kV high voltage, 20 cm spinneret - collector distance, aluminium foil collector, 23 ℃ ambient temperature and 39 % air humidity.

2.3.Materials characterization

The samples morphology and elemental composition were investigated by scanning electron microscopy (SEM), with a Quanta Inspect F microscope (FEI Company, Hillsboro, OR, USA) equipped with energy-dispersive X-ray spectroscopy (EDS) probe, as well as dynamic light scattering (DLS), with a DelsaMax Pro equipment (Beckman Coulter, Brea, CA, USA). To ensure conductive surfaces for the SEM evaluation, the samples were coated with a thin layer of gold by DC magnetron sputtering; during operation, the electron beam was accelerated under a voltage of 30 kV, having a spot size of 3.5. For the DLS experiments, 4 mg of powder were dispersed in 12 mL ultrapure water by ultrasonication for 10 min; two measurements on different specimens from the same sample were conducted. In order to elucidate the phase composition and crystal structure, X-ray diffraction (XRD) was also performed, with a Shimadzu XRD 6000 diffractometer (Shimadzu Corporation, Kyoto, Japan), employing Ni-filtered Cu Kα radiation (λ = 1.54 Å); 2θ was ranged between 20 and 70 °, with a scan speed of 2 °/min and a step size of 0.02 °.

2.4.Biological characterization

Mouse fibroblast cells L929 were grown in MEM supplemented with 2 mM L-Glutamine, 10 % fetal calf serum (FCS), 100 units/mL of penicillin, and 100 μg/mL of streptomycin, at 37 °C, in a humidified incubator, under an atmosphere containing 5 % CO_2. All cell cultivation media and reagents were purchased from Biochrom AG (Berlin, Germany).

Cell viability was evaluated using 3-(4,5-dimethylthiazol-2-yl)-2,5-diphenyltetrazolium bromide (MTT) assay at 24 and 48 h after the cells were seeded onto the analysed fibrous scaffolds. Briefly, the surfaces were sterilized in flow with UV light, 15 min on each side. Following the sterilization, 1 cm^2 squares were placed in 24-well plates and seeded with 20.000 cells/well for 24 and 48 h. After the desired time passed, the medium was exchanged with medium containing MTT and further incubated for 4 h in the incubator. Finally, the solution was extracted and the formed crystals were dissolved in dimethyl sulfoxide (DMSO). Negative control was represented by cells cultivated only in medium on aluminium foil. The percentage of viable cells was obtained using Equation (1).

$$Cell\ viability = [(A_{570} of\ treated\ cells)/(A_{570} of\ untreated\ cells)] \times 100\ (\%) \quad (1)$$

Fluorescence microscopy was used to investigate the cellular morphology of L929 cells grown for 24 h on the prepared materials. The cells were grown as described above for 24 h, then washed with PBS, fixed in 4 % paraformaldehyde dissolved in PBS for 15 min, and washed again with PBS for 15 min. Further, the cells were stained with Acridine Orange (20 μg/mL) for 15 min and washed

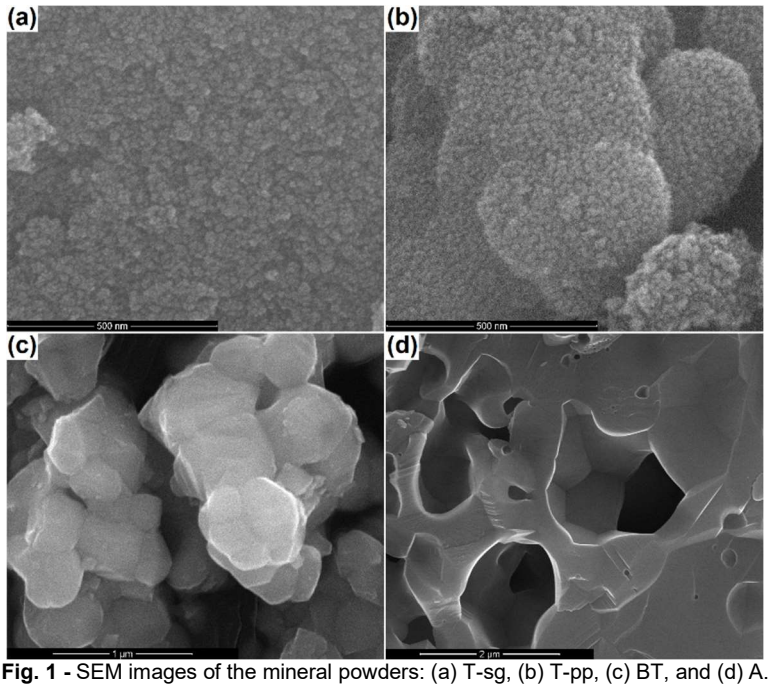

Fig. 1 - SEM images of the mineral powders: (a) T-sg, (b) T-pp, (c) BT, and (d) A.
Imagini SEM ale pulberilor minerale: (a) T-sg, (b) T-pp, (c) BT și (d) A.

again with PBS. Finally, the samples were mounted on glass slides, and the fluorescence images were recorded using a disc scanning confocal microscope (Andor DSD2 Confocal Unit, Belfast, UK) mounted on an Olympus BX51 epifluorescence microscope, equipped with a 40× objective. A suitable filter cube (excitation filter 466/40 nm, dichroic mirror 488 nm, and emission filter 525/54 nm) was employed for the acquisition of the images.

3. Results and discussion

The features of the mineral powders employed as decorations are shown in Fig. 1. Both TiO_2 powders (T-sg and T-pp) are nanosized, with quasi-spherical particles gathered in micrometric agglomerates; the particle size estimation led to values below 10 nm, maybe slightly higher for the sol-gel method (Fig. 1a *vs.* Fig. 1b). BT powder, a valuable piezoelectric ceramic [41-43], corresponds to the description provided by the supplier, consisting of polyhedral pieces with dimensions below 3 µm, sometimes tightly packed in bunches (Fig. 1c). Going to the silicate powder, it is obvious that the applied temperature of 1300 °C enabled a partial sintering, fact that promoted the occurrence of porous bodies of several micrometres, in which the boundaries between large, rounded grains are clearly visible (Fig. 1d). Basically, powdery systems consisting of entities with sizes ranging from several nanometers to few microns were selected as inorganic phases for studying both the morphological impact on PVDF fibre formation through electrospinning and the effect of such combinations on the cellular behaviour at short stages.

For an overview of the previously approached powders, DLS experiments were conducted, the results being listed in Table 1. According to the size evaluation performed by optical means, the particle diameter is quite different for the two TiO_2 samples, namely a diameter at least double for T-pp compared to T-sg; however, this result can be an artifact if we consider that the aggregates made of nanoparticles are difficult to split due to their high surface energy that can be reduced only by creating clusters. The value obtained in the case of BT powder is compatible with the information given in the product sheet, as well as the SEM observations. A surprising diameter was achieved only for A sample, below 1 µm, which suggests that the application of ultrasounds before analysis has a pronounced repercussion on the disintegration of the noticed micrometric porous bodies. The values of Zeta potential place all powders in the area of instability, while the polydispersity index reveals a larger size distribution for A powder, bimodal and asymmetric.

The inorganic loadings were also investigated from a structural point of view (Fig. 2). The associated XRD patterns indicate single phase and tetragonal symmetry for both TiO_2 (ICDD 00-084-1286) and BT (ICDD 00-081-2201). It can be observed that a very small quantity of secondary phase appears in the case of T-sg, namely another type of order in TiO_2 (rutile as against anatase, ICDD 00-084-1284). The silicate powder consists of four crystalline phases, all in high proportions and with well-known bioactive potential [44]: tetragonal akermanite ($Ca_2MgSi_2O_7$, ICDD 00-083-1815), monoclinic merwinite ($Ca_3MgSi_2O_8$, ICDD 00-074-0382), monoclinic diopside ($CaMgSi_2O_6$, ICDD 00-083-1817) and monoclinic calcium disilicate

Table 1

Hydrodynamic diameter, Zeta potential, and polydispersity index of the mineral powders, extracted from the dynamic light scattering experiments / *Diametrul hidrodinamic, potențialul Zeta și indicele de polidispersitate ale pulberilor minerale, extrase din experimentele de împrăștiere dinamică a luminii.*

Powder	Hydrodynamic diameter (nm)	Zeta potential (mV)	Polydispersity index
T-sg	608.15 ± 11.24	25.82 ± 0.44	0.23 ± 0.01
T-pp	1467.60 ± 159.24	21.64 ± 1.70	0.10 ± 0.12
BT	960.00 ± 12.45	–22.38 ± 0.13	0.16 ± 0.01
A	737.60 ± 35.50	–26.35 ± 1.34	0.57 ± 0.00

(Ca_2SiO_4, ICDD 00-083-0464, ICDD 00-083-2457). Even though the synthesis started from the oxide composition of akermanite, the reactions that occurred at high temperatures enabled the formation of binary or ternary compounds, the difficulty of obtaining single-phase in such cases being well-known.

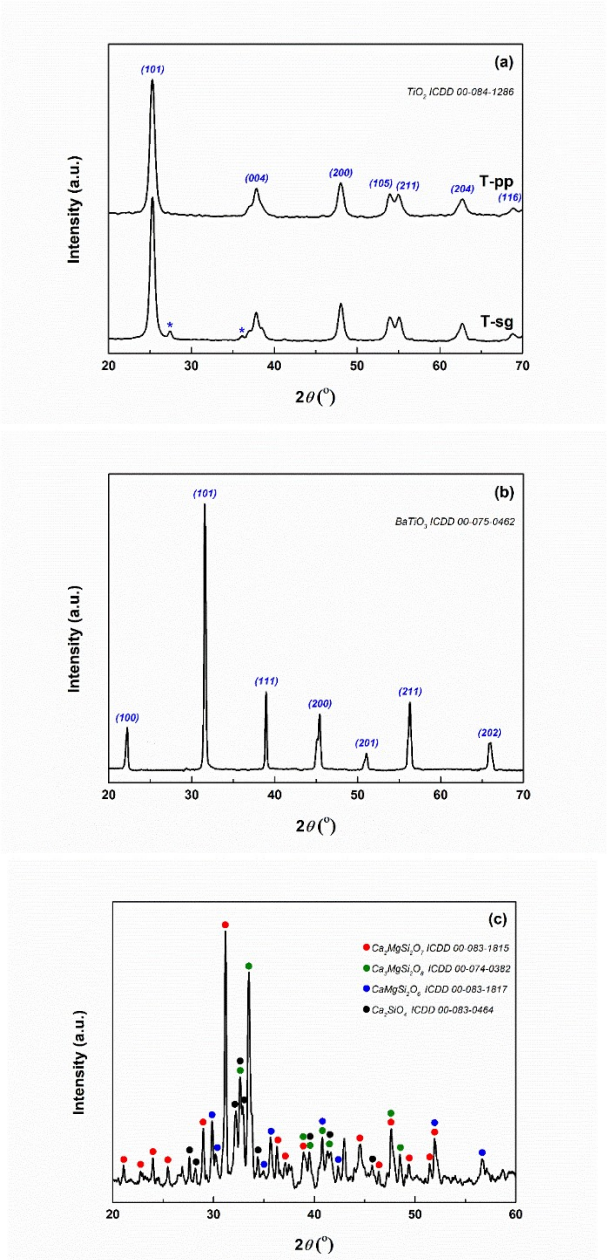

Fig. 2 - XRD patterns of the mineral powders: (a) T, (b) BT, and (c) A. */ Analizele XRD ale pulberilor minerale: (a) T, (b) BT și (c) A.*

In Fig. 3a, non-woven networks of fibres, arranged randomly, with various diameters (between 100 and 1000 nm) and fusiform entities in places can be distinguished. The number of beads is probably reduced due to the application of a high voltage of 18 kV. The addition of mineral powders into the electrospinning solutions caused significant changes in terms of scaffold morphology (Figs. 3b-e). In the case of T-sg powder (Fig. 3b), the fibres mostly embed agglomerations of TiO_2 particles, which is not beneficial for expressing their antibacterial activity [45], the active surface being blocked. However, T-pp powder (Fig. 3c) is localized as agglomerations of TiO_2 particles between PVDF fibres, which is desirable for the final application, namely the limitation of bacteria growth and reproduction. In both cases, the powder distribution appears to be quite homogeneous over large areas. Arif *et al.* [1] employed 0.005, 0.01, and 0.02 g TiO_2 with anatase phase per 1 g of PVDF, the powder being incorporated in the polymeric membrane; the corresponding samples exhibited excellent antimicrobial properties against Gram-negative *E. coli*. In our case, the weight ratio between PVDF and TiO_2 was 20:3, namely 0.15 g TiO_2 per 1 g of PVDF, which means a much higher content of inorganic powder in the resulting fibrous scaffolds. Taking into account the fact that some of the particles can sediment gravitationally in the syringe before being expelled in the electric field, the real concentration of the discontinuous phase may be significantly lower than the designed one. Nevertheless, it is expected to achieve a good response in terms of antibacterial activity even in these conditions.

The addition of BT powder (Fig. 3d) leads to a network that includes BT particles in a manner that does not affect the fibre continuity and does not dramatically change its diameter (300 - 900 nm). A much better spatial dispersion and a narrower size distribution of the mineral clusters seem to be reached, maybe because the efficiency of the applied ultrasounds in the homogenization stage was higher than in the case of the nanosized powders. Almeida *et al.* [36] used three different sizes of commercial BT powder and set the weight ratio between PVDF and BT at 6:1, 4:1, and 3:1; considering the closest concentration to ours (6:1), the electrospun composite fibres displayed an average diameter of 0.7 μm, which is quite similar to the results in this paper, but also the highest percentage of living cells at the cytotoxicity analysis.

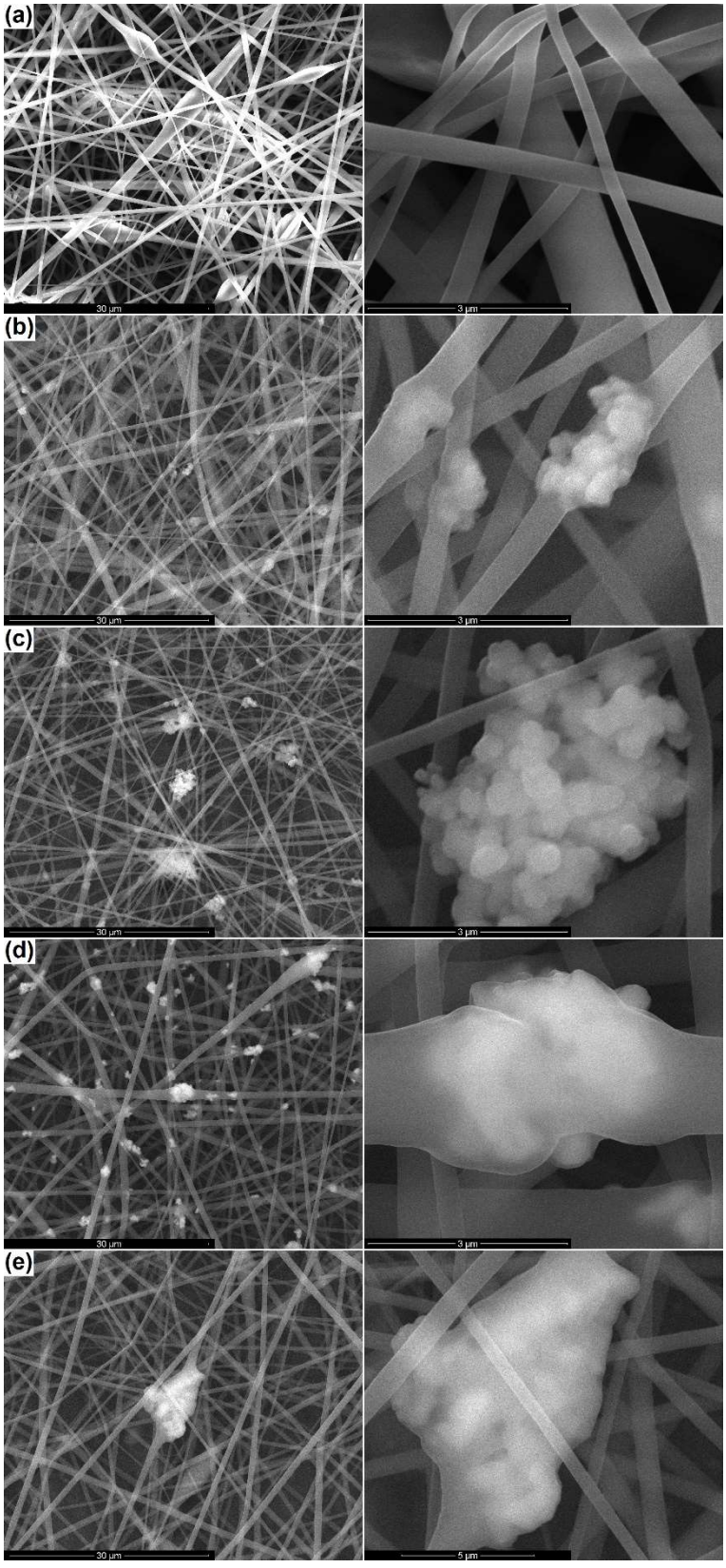

Fig. 3 - SEM images of the electrospun samples with 3 % powder loading: (a) PVDF, (b) PVDF-T-sg (c) PVDF-T-pp, (d) PVDF-BT and (e) PVDF-A.
Imagini SEM ale probelor electrofilate cu încărcare de 3 % pulbere: (a) PVDF, (b) PVDF-T-sg (c) PVDF-T-pp, (d) PVDF-BT și (e) PVDF-A.

Moreover, the authors also showed that BT particles hinder the alignment of PVDF in the fibres, a fact that could alter the piezoelectric properties.

Akermanite powder (Fig. 3e) is found both inside and outside the fibre because the high processing temperature favored the formation of large, sintered blocks. However, the fibres are not interrupted and have constant diameters over long distances (400 - 900 nm). Moreover, the beads do not disappear completely, being sometimes confused with the diameter increase given by the powder inclusion. The inorganic phase is present to a lesser degree, an aspect that was expectable to a certain extent since the large volume of Ak entities stimulates their deposition at the bottom of the syringe, making impossible their further embedding in the fibres. Though, anchoring of some bioactive blocks at the surface of PVDF fibres could ensure active areas for fast mineralization when introduced in simulated body fluids or living organisms.

The EDX spectra recorded on the plain PVDF fibres, as well as those combined with inorganic powders (Fig. 4) highlight the common elements, namely: C, F, O (fluoropolymer), Al (collecting foil), and Au (coating for SEM analysis). Considering the EDX spectra made on network areas having obvious decorations with different types of aggregates, Ti, Ba, Ca, Mg, and Si elements also appear, as proof of the successful fibre loading.

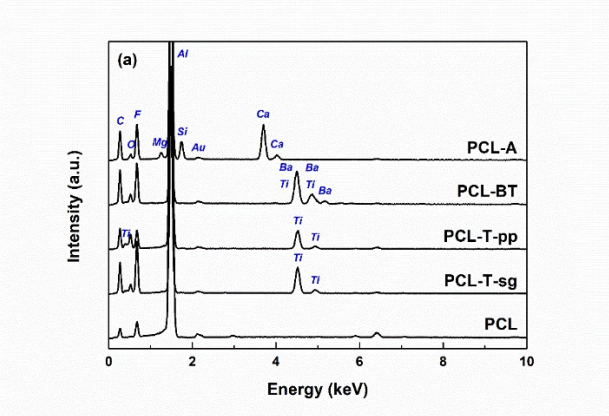

Fig. 4 - EDX spectra of the electrospun samples with 3 % powder loading / *Spectrele EDX ale probelor electrofilate cu încărcare de 3 % pulbere*.

After the cellular testing, it was found that the proposed scaffolds are not cytotoxic and sustain cell proliferation. Thus, the cell viability of PVDF-T-sg, PVDF-BT, and PVDF-A grew with the increase in seeding time, while PVDF-T-pp presented a slightly lower value after 48 h, as can be seen in Fig. 5. Overall, the response given by the composite

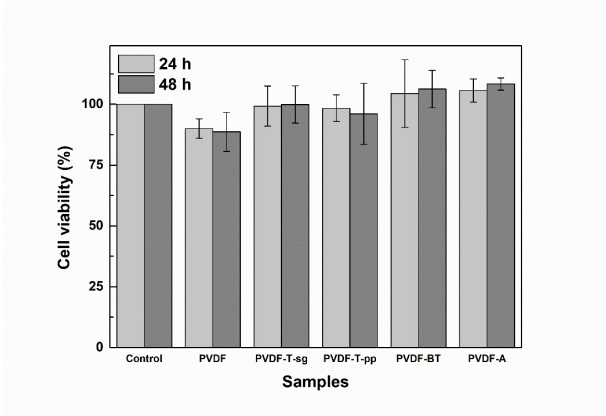

Fig. 5 - Cell viability for fibroblast cells in contact with the electrospun samples for 24 and 48 h.
Viabilitatea celulară pentru celule fibroblaste în contact cu probele electrofilate timp de 24 și 48 h.

samples is superior to the one displayed by the polymeric network, which encourages the continuation of this study in order to extend the biological characterization.

The fluorescence images of L929 cells grown on the analysed samples are presented in Fig. 6; these were used to investigate cell morphology, adhesion, and spreading on the surface, the interaction between cells and material also indicating its biocompatibility. Cell attachment to other cells or surfaces plays an important role in cellular processes and signalling, like cell growth, division, and migration [46, 47]. Depending on the surface properties, the attachment and spreading of the cells can vary from conditions that favor the development of the cells, found for biocompatible materials, to ones where the cells exhibit rounded and shrank morphology, indicating a surface to which the cells show less affinity [48-51]. The images recorded for fibroblast cells grown on glass slides (Control conditions) exhibit their characteristic morphology: a large, oval nucleus and a spindle shape cell body with the size between 20 and 30 μm (Fig. 6A). When it comes to the prepared scaffolds, L929 cells displayed a good attachment to the corresponding surfaces after 24 h, with the typical morphology of the Control cells, independent of the surface composition (Figs. 6B-F). Based on the morphological features of the investigated cells, it can be stated that the images reveal similar results to those previously reported for cell viability. Thus, the results indicate that independent of the sample characteristics, all developed materials have good biocompatibility concerning L929 cells.

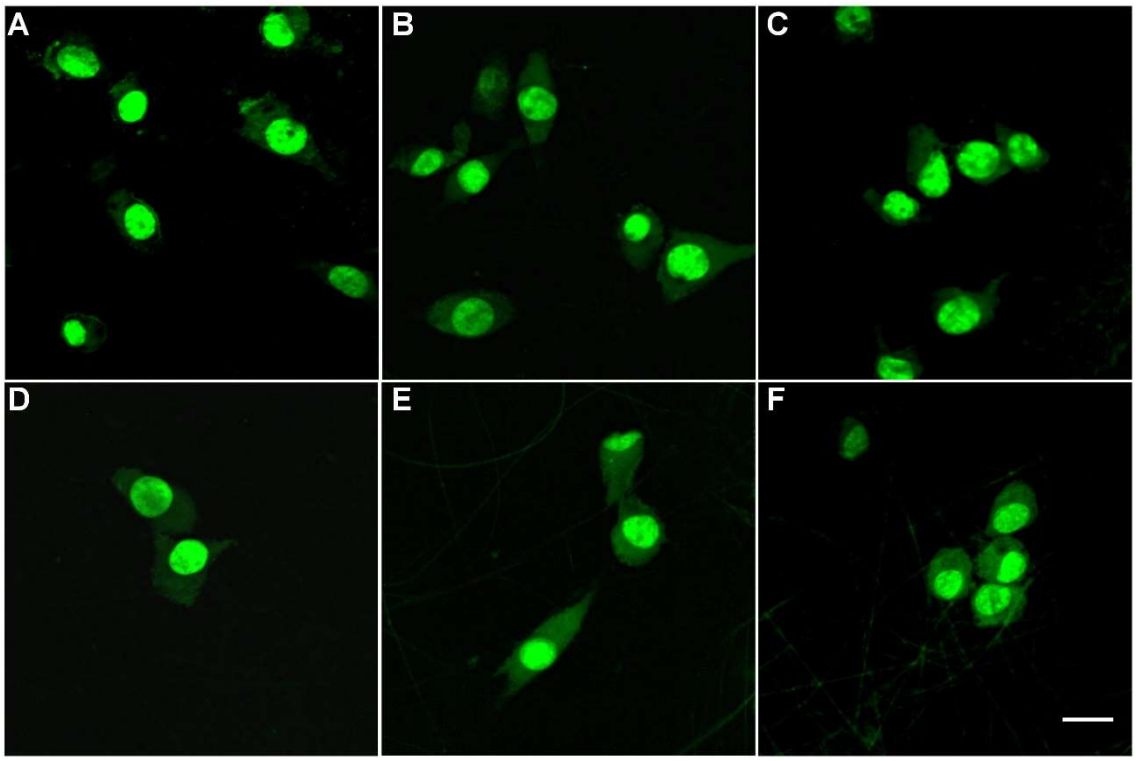

Fig. 6 - Morphological evaluation of fibroblast cells in contact with the samples for 24 h:
(A) Control, (B) PVDF, (C) PVDF-T-sg, (D) PVDF-T-pp, (E) PVDF-BT and (F) PVDF-A.
The scale bar is 20 μm and the same for all images. / *Evaluarea morfologică a celulelor fibroblaste în contact cu probele timp de 24 h:*
(A) Control, (B) PVDF, (C) PVDF-T-sg, (D) PVDF-T-pp, (E) PVDF-BT și (F) PVDF-A.
Scala este de 20 μm și este aceeași pentru toate imaginile.

4. Conclusions

Using the electrospinning method, composite fibre networks based on polyvinylidene fluoride were successfully produced, these being loaded with mineral powders with the aim of fabricating scaffolds with suitable properties for application in tissue engineering. The inorganic components were represented by titanium dioxide, barium titanate, and calcium magnesium silicate, motivated by the possibility of conferring additional properties: antibacterial activity (titanium dioxide) enhanced piezoelectric properties (barium titanate), or bioactivity (calcium magnesium silicate). Following the analyses carried out on the obtained composites, it can be stated that they show good homogeneity in terms of loading with inorganic powders, these being arranged both inside the fibres and suspended at the intersection between several fibres. The final materials present a morphology that facilitates the penetration of cells inside the scaffold due to the degree of porosity and pore size, this being beneficial in the targeted applications. Nevertheless, it should be noted that the samples based on PVDF and BT particles have a different appearance, the corresponding fibres being a little thicker and their continuity not being modified by the embedded aggregates. The viability of fibroblast cells contacted with the composites was always higher than that of PVDF fibres, demonstrating the potential of these materials to be integrated into tissue engineering devices as multifunctional components.

Acknowledgments

This work was supported by the grant POCU/993/6/13–153178, co-financed by the European Social Fund within the Sectorial Operational Program Human Capital 2014–2020. M.B. and M.R. acknowledge the financial support of the Nucleu Programme at IFIN-HH, Contract No. PN 19 06 02 03/2019.

REFERENCES

[1] Arif, Z.; Seth, N.K.; Kumari, L.; Mishra, P.K.; Verma, B. Antifouling behaviour of PVDF/TiO_2 composite membrane: A quantitative and qualitative assessment. *Iran. Polym. J.* 2019, **28**, 301–312.

[2] Tandon, B.; Kamble, P.; Olsson, R.T.; Blaker, J.J.; Cartmell, S.H. Fabrication and characterisation of stimuli responsive piezoelectric PVDF and hydroxyapatite-filled PVDF fibrous membranes. *Molecules* 2019, **24**, 1903.

[3] Braga, F.J.C.; Rogero, S.O.; Couto, A.A.; Marques, R.F.C.; Ribeiro, A.A.; Carvalho Campos, J.S. Characterization of PVDF/HAP composites for medical applications. *Mater. Res.* 2007, **10**, 247–251.

[4] dos Santos, G.G.; Malherbi, M.S.; de Souza, N.S.; Cesar, G.B.; Tominaga, T.T.; Miyahara, R.Y.; de Mendonca, P.d.S.B.; Faria, D.R.; Rosso, J.M.; Freitas, V.F.; Weinand, W. R.; Dias, G.S.; Santos, I.A.; Cotica, L.F. Generation biomaterials based on PVDF-hydroxyapatite composites produced by electrospinning: Processing and characterization. *Polymers* 2022, **14,** 4190.

[5] Sakarkar, S.; Muthukumaran, S.; Jegatheesan, V. Tailoring the effects of titanium dioxide (TiO_2) and polyvinyl alcohol (PVA) in the separation and antifouling performance of thin-film composite polyvinylidene fluoride (PVDF) membrane. *Membranes* 2021, **11**, 241.

[6] Alecu, A.E.; Girjoaba, S.A.; Beregoi, M.; Jinga, S.I.; Busuioc, C. The influence of electrospinning parameters on the morphological features of PVDF fibres. *Rom. J. Mater.* 2022, **52**, 228–237.

[7] Venkatraman, S.K.; Swamiappan, S. Review on calcium- and magnesium-based silicates for bone tissue engineering applications. *J. Biomed. Mater. Res. A* 2020, **108**, 1546–1562.
[8] Toshev, O.; Safronova, T.; Kaimonov, M.; Shatalova, T.; Klimashina, E.; Lukina, Y.; Malyutin, K.; Sivkov, S. Biocompatibility of ceramic materials in $Ca_2P_2O_7$-$Ca(PO_3)_2$ system obtained via heat treatment of cement-salt stone. *Ceramics* 2022, **5**, 516–532.
[9] Dorozhkin, S.V. Calcium orthophosphate ($CaPO_4$)-based bioceramics: Preparation, properties, and applications. *Coatings* 2022, **12**, 1380.
[10] Habib, S.; Rashid, F.; Tahir, H.; Liaqat, I.; Latif, A.A.; Naseem, S.; Khalid, A.; Haider, N.; Hani, U.; Dawoud, R.A.; Modafer, Y.; Bibi, A.; Jefri, O.A. Antibacterial and cytotoxic effects of biosynthesized zinc oxide and titanium dioxide nanoparticles. *Microorganisms* 2023, **11**, 1363.
[11] Polley, C.; Distler, T.; Detsch, R.; Lund, H.; Springer, A.; Boccaccini, A.R.; Seitz, H. 3D printing of piezoelectric barium titanate-hydroxyapatite scaffolds with interconnected porosity for bone tissue engineering. *Materials* 2020, **13**, 1773.
[12] Busuioc, C.; Voicu, G.; Jinga, S.I.; Mitran, V.; Cimpean, A. The influence of barium titanate on the biological properties of collagen-hydroxiapatite composite scaffolds. *Materials Letters* 2019, **253**, 317–322.
[13] Busuioc, C.; Alecu, A.E.; Costea, C.C.; Beregoi, M.; Bacalum, M.; Raileanu, M.; Jinga, S.I.; Deleanu, I.M. Composite fibers based on polycaprolactone and calcium magnesium silicate powders for tissue engineering applications. *Polymers* 2022, **14**, 4611.
[14] Stabler, S.M.; Henry, J.; Chauveau, J. Polyvinylidene fluoride fibres for multiple high performance uses. *Filtr. Sep.* 2014, **51**, 42–45.
[15] Dallaev, R.; Pisarenko, T.; Sobola, D.; Orudzhev, F.; Ramazanov, S.; Trcka, T. Brief review of PVDF properties and applications potential. *Polymers* 2022, **14**, 4793.
[16] He, Z.; Rault, F.; Lewandowski, M.; Mohsenzadeh, E.; Salaun, F. Electrospun PVDF nanofibers for piezoelectric applications: A review of the influence of electrospinning parameters on the phase and crystallinity enhancement. *Polymers* 2021, **13**, 174.
[17] Pisarenko, T.; Papez, N.; Sobola, D.; Talu, S.; Castkova, K.; Skarvada, P.; Macku, R.; Scasnovic, E.; Kastyl, J. Comprehensive characterization of PVDF nanofibers at macro- and nanolevel. *Polymers* 2022, **14**, 593.
[18] Aghayari, S. An introduction to PVDF nanofibers properties, and ways to improve them, and reviewing output enhancing methods for PVDF nanofibers nanogenerators. *Preprints* 2021, 2021110380.
[19] Zaarour, B.; Wanjun, L. Enhanced piezoelectric performance of electrospun PVDF nanofibers by regulating the solvent systems. *J. Eng. Fibers Fabr.* 2022, **17**, 1–8.
[20] He, Z.; Rault, F.; Lewandowski, M.; Mohsenzadeh, E.; Salaun, F. Electrospun PVDF nanofibers for piezoelectric applications: A review of the influence of electrospinning parameters on the *β* phase and crystallinity enhancement. *Polymers* 2021, **13**, 174.
[21] Mohammadpourfazeli, S.; Arash, S.; Ansari, A.; Yang, S.; Mallick, K.; Bagherzadeh, R. Future prospects and recent developments of polyvinylidene fluoride (PVDF) piezoelectric polymer; fabrication methods, structure, and electro-mechanical properties. *RSC Adv.* 2023, **13**, 370.
[22] Kalimuldina, G.; Turdakyn, N.; Abay, I.; Medeubayev, A.; Nurpeissova, A.; Adair, D.; Bakenov, Z. A review of piezoelectric PVDF film by electrospinning and its applications. *Sensors* 2020, **20**, 5214.
[23] Azimi, B.; Milazzo, M.; Lazzeri, A.; Berrettini, S.; Uddin, M.J.; Qin, Z.; Buehler, M.J.; Danti, S. Electrospinning piezoelectric fibers for biocompatible devices. *Adv. Healthc. Mater.* 2020, **9**, e1901287.
[24] Zhang, W.; Wu, G.; Zeng, H.; Li, Z.; Wu, W.; Jiang, H.; Zhang, W.; Wu, R.; Huang, Y.; Lei, Z. The preparation, structural design, and application of electroactive poly(vinylidene fluoride)-based materials for wearable sensors and human energy harvesters. *Polymers* 2023, **15**, 2766.
[25] Sobreiro-Almeida, R.; Tamano-Machiavello, M.N.; Carvalho, E.O.; Cordon, L.; Doria, S.; Senent, L.; Correia, D.M.; Ribeiro, C.; Lanceros-Mendez, S.; Sabater i Serra, R.; Gomez Ribelles, J.L.; Sempere, A. Human mesenchymal stem cells growth and osteogenic differentiation on piezoelectric poly(vinylidene fluoride) microsphere substrates. *Int. J. Mol. Sci.* 2017, **18**, 2391.
[26] Chang, H.M.; Zhan, W.P.; Tsai, H.C.; Yang, M.R. Poly(vinylidene fluoride) intestinal sleeve implants for the treatment of obesity and type 2 diabetes. *Polymers* 2022, **14**, 2178.
[27] Pan, C.T.; Dutt, K.; Kumar, A.; Kumar, R.; Chuang, C.H.; Lo, Y.T.; Wen, Z.H.; Wang, C.S.; Kuo, S.W. PVDF/AgNP/MXene composites-based near-field electrospun fiber with enhanced piezoelectric performance for self-powered wearable sensors. *Int. J. Bioprinting* 2022, **9**, 647.
[28] Nguyen, D.N.; Moon, W. Fabrication and characterization of a flexible PVDF fiber-based polymer composite for high-performance energy harvesting devices. *J Sens. Sci. Technol.* 2019, **28**, 205–215.
[29] Lolla, D.; Pan, L.; Gade, H.; Chase, G.G. Functionalized polyvinylidene fluoride electrospun nanofibers and applications. In *Electrospinning Method Used to Create Functional Nanocomposites Films*; Tanski, T.; Jarka. P.; Matysiak, W., Eds.; InTech: London, UK, 2018; Chapter 5, pp. 70–89.
[30] Mokhtari, F.; Latifi, M.; Shamshirsaz, M. Applying the genetic algorithm for determination electro spinning parameters of poly vinylidene fluoride (PVDF) nano fibers: Theoretical & experimental analysis. *J. Textile Eng. Fashion Technol.* 2017, **3**, 640–648.
[31] Castkova, K.; Kastyl, J.; Sobola, D.; Petrus, J.; Stastna, E.; Riha, D.; Tofel, P. Structure-properties relationship of electrospun PVDF fibers. *Nanomaterials* 2020, **10**, 1221.
[32] Issa, A.A.; Al-Maadeed, M.A.; Luyt, A.S.; Ponnamma, D.; Hassan, M.K. Physico-mechanical, dielectric, and piezoelectric properties of PVDF electrospun mats containing silver nanoparticles. *C* 2017, **3**, 30.
[33] Sta. Agueda, J.R.; Madrid, J.; Mondragon, J.M.; Lim, J.; Tan, A.; Wang, I.; Duguran, N.; Bondoc, A. Synthesis and characterization of electrospun polyvinylidene fluoride-based (PVDF) scaffolds for renal bioengineering. *J. Phys. Conf. Ser.* 2021, **2071**, 012005.
[34] Li, C.; Yu, H.; Huang, B.; Liu, G.; Guo, Y.; Zhu, H.; Yu, B. Fabrication of anatase TiO_2/PVDF composite membrane for oil-in-water emulsion separation and dye photocatalytic degradation. *Membranes* 2023, **13**, 364.
[35] Su, Y.P.; Sim, L.N.; Coster, H.G.L.; Chong, T.H. Incorporation of barium titanate nanoparticles in piezoelectric PVDF membrane. *J. Membr. Sci.* 2021, **640**, 119861.
[36] Almeida, S.D.; Silva, J.C.; Borges, J.P.M.R.; Lança, M.C. Characterization of a biocomposite of electrospun PVDF membranes with embedded $BaTiO_3$ micro- and nanoparticles. *Macromol*. 2022, **2**, 531–542.
[37] Rodrigues, P.J.G.; de M.V. Elias, C.; Viana, B.C.; de Hollanda, L.M.; Stocco, T.D.; de Vasconcellos, L.M.R.; de C.R. Mello, D.; Santos, F.E.P.; Marciano, F.R.; Lobo, A.O. Electrodeposition of bactericidal and bioactive nano-hydroxyapatite onto electrospun piezoelectric polyvinylidene fluoride scaffolds. *J. Mater. Res.* 2020, **35**, 3265–3275.
[38] Xu, Q.; Chen, Y.; Xiao, T.; Yang, X. A Facile method to control pore structure of PVDF/SiO_2 composite membranes for efficient oil/water purification. *Membranes* 2021, **11**, 803.

[39] Alecu, A.E.; Girjoaba, S.A.; Enculescu, M.M.; Busuioc, C. Comparative study on TiO_2 nanoparticles obtained by precipitation and sol-gel. *U.P.B. Sci. Bull.* 2023, **85**, 117–128.

[40] Alecu, A.E.; Costea, C.C.; Surdu, V.A.; Voicu, G.; Jinga, S.I.; Busuioc, C. Processing of calcium magnesium silicates by the sol-gel route. *Gels* 2022, **8**, 574.

[41] Joseph, N.; Singh, S.K.; Sirugudu, R.K.; Murthy, V.R.K.; Ananthakumar, S.; Sebastian, M.T. Effect of silver incorporation into PVDF-barium titanate composites for EMI shielding applications. *Mater. Res. Bull.* 2013, **48**, 1681–1687.

[42] Song, S.; Li, Y.; Wang, Q.; Zhang, C. Facile preparation of high loading filled PVDF/$BaTiO_3$ piezoelectric composites for selective laser sintering *3D* printing. *RSC Adv.* 2021, **11**, 37923.

[43] Wang, Y.; Yao, M.; Ma, R.; Yuan, Q.; Yang, D.; Cui, B.; Ma, C.; Liu, M.; Hu, D. Design strategy of barium titanate/polyvinylidene fluoride-based nanocomposite films for high energy storage. *J. Mater. Chem. A* 2020, **8**, 884–917.

[44] Collin, M.S.; Venkatraman, S.K.; Mohana, S.; Sumathi, S.; Drweesh, E.A.; Elnagar, M.M.; Mosa, E.S.; Sasikumar, S. Solution combustion synthesis of functional diopside, akermanite, and merwinite bioceramics: Excellent biomineralization, mechanical strength, and antibacterial ability. *Mater. Today Commun.* 2021, **27**, 102365.

[45] Kubacka, A.; Diez, M.S.; Rojo, D.; Bargiela, R.; Ciordia, S.; Zapico, I.; Albar, J.P.; Barbas, C.; Martins dos Santos, V.A.P.; Fernandez-Garcia, M.; Ferrer, M. Understanding the antimicrobial mechanism of TiO_2-based nanocomposite films in a pathogenic bacterium. *Sci. Rep.* 2014, **4**, 4134.

[46] Khalili, A.A.; Ahmad, M.R. A review of cell adhesion studies for biomedical and biological applications. *Int. J. Mol. Sci.* 2015, **16**, 18149–18184.

[47] Pugacheva, E.N.; Roegiers, F.; Golemis, E.A. Interdependence of cell attachment and cell cycle signaling. *Curr. Opin. Cell Biol.* 2006, **18**, 507–515.

[48] Majhy, B.; Priyadarshini, P.; Sen, A.K. Effect of surface energy and roughness on cell adhesion and growth - facile surface modification for enhanced cell culture. *RSC Adv.* 2021, **11**, 15467–15476.

[49] Lotfi, M.; Nejib, M.; Naceur, M. Cell adhesion to biomaterials: Concept of biocompatibility. In *Advances in Biomaterials Science and Biomedical Applications*; Pignatello, R., Ed.; InTech: London, UK, 2013; Chapter 8, pp. 207–240.

[50] Lavenus, S.; Pilet, P.; Guicheux, J.; Weiss, P.; Louarn, G.; Layrolle, P. Behaviour of mesenchymal stem cells, fibroblasts and osteoblasts on smooth surfaces. *Acta Biomater.* 2011, **7**, 1525–1534.

[51] Paino, F.; Ricci, G.; De Rosa, A.; D'Aquino, R.; Laino, L.; Pirozzi, G.; Tirino, V.; Papaccio, G. Ecto-mesenchymal stem cells from dental pulp are committed to differentiate into active melanocytes. *Eur. Cell. Mater.* 2010, **20**, 295–305.

****